 Nucleic Acids Research, 1999, Vol. 27, No. 21 **4261–4268**

NMR solution structure of a DNA dodecamer containing a transplatin interstrand GN7–CN3 cross-link

Françoise Paquet*, Marc Boudvillain, Gérard Lancelot and Marc Leng

Centre de Biophysique Moléculaire, CNRS–UPR 4301, Rue Charles Sadron, F-45071 Orleans Cédex 2, France

Received June 9, 1999; Revised August 10, 1999; Accepted September 14, 1999

ABSTRACT

The DNA duplex d(CTCTCG*AGTCTC)·d(GAGAC-TC*GAGAG) containing a single *trans*-diammine-dichloroplatinum(II) interstrand cross-link (where G* and C* represent the platinated bases) has been studied by two-dimensional NMR. All the exchange-able and non-exchangeable proton resonance lines were assigned (except H5′/H5″) and the NOE intensities were transformed into distances via the RELAZ program. By combining the NOESY and COSY data (330 constraints) and NMR-constrained molecular mechanics using JUMNA, a solution structure of the cross-linked duplex has been determined. The duplex is distorted over two base pairs on each side of the interstrand cross-link and exhibits a slight bending of its axis (~20°) towards the minor groove. The platinated guanine G* adopts a *syn* conformation. The rotation results in a Hoogsteen-type pairing between the complementary G_6* and C_{19}* residues which is mediated by the platinum moiety and is stabilized by a hydrogen bond between O6(G_6*) and N4H(C_{19}*). The rise between the cross-linked residues and the adjacent residues is increased owing to the interaction between these adjacent residues and the ammine groups of the platinum moiety. These results are discussed in relation to the slow rate of closure of the monofunctional adducts into interstrand cross-links.

INTRODUCTION

cis-diamminedichloroplatinum(II) (cisplatin) is one of the most widely used drugs for the treatment of human cancers. Cisplatin triggers cell death by apoptosis but its complete mechanism of action as well as the way cells develop resistance to the drug are not yet elucidated (1–3). It is generally accepted that the target of cisplatin is cellular DNA. The major lesions formed in the reaction between cisplatin and DNA are 1,2-intrastrand cross-links between adjacent purine residues. Interstrand cross-links are minor lesions and are preferentially formed between two guanine residues on opposite strands at d(GpC)·d(GpC) sites (4–6). Although the recently reported specific recognition of cisplatin-modified DNA at d(PupPu) sites by several proteins gives strong support for the hypothesis of a key role played by the major 1,2-intrastrand cross-links (7) one cannot totally exclude a role of the interstrand cross-links (8).

The systematic study of platinum complexes led to empirical pharmacological structure–activity relationships. The complexes must have the *cis* conformation since *trans*-diamminedichloro-platinum(II) (transplatin), the stereoisomer of cisplatin, is clinically inactive. For steric reasons, transplatin cannot form intrastrand cross-links between adjacent purine residues which could explain its inefficiency (4,6). However, recent studies have shown that several complexes with *trans* geometry for the leaving groups have antitumor activity and are able to over-come cisplatin resistance of cancer cells (9–14).

Numerous studies support the hypothesis that the formation of adducts in the reaction between DNA and cisplatin or trans-platin proceeds in two successive solvent-assisted reactions (4–6). Both compounds react preferentially with G residues and form monofunctional adducts. The cisplatin monofunctional adducts react further and form bifunctional adducts within a few hours. Closure of the transplatin monofunctional adducts is at least 10 times slower and results mainly in the formation of inter-strand cross-links (15). Intrastrand cross-links, if formed, are rare products (16,17). Another major difference between cisplatin and transplatin is that in the interstrand lesions transplatin cross-links complementary G and C residues (15). Interestingly, G–C interstrand cross-links also result from the rearrangement of (G1,G3) interstrand cross-links triggered by the pairing of single-stranded transplatin-modified oligonucleotides with their complementary strands (8).

The distortions induced in the DNA double helix by cisplatin interstrand cross-links have been studied by several approaches (8) including recent NMR and crystallographic studies (18–20). In contrast, the distortions induced by transplatin interstrand cross-links have only been described by means of gel electrophoresis, chemical probes and molecular modeling (21). From these studies it has been inferred that the double helix is distorted on both sides of the cross-link but that the bases are still paired. The double helix is unwound by ~12° and its axis is bent by ~26°.

Taking into account the promising clinical applications of new platinum complexes having the *trans* geometry, the need for a complete explanation of the clinical inefficiency of trans-platin, the induced rearrangement of transplatin (G1,G3) intrastrand cross-links into interstrand cross-links and the unexpected difference in the nature of the bases cross-linked by cisplatin and transplatin, it appeared to us of importance to give a detailed description of the distortions induced in DNA

*To whom correspondence should be addressed. Tel: +33 2 38 25 76 92; Fax: +33 2 38 63 15 17; Email: paquet@cnrs-orleans.fr

by transplatin interstrand cross-links. In this paper we report the solution structure of a double-stranded oligonucleotide d(CTCTCG*AGTCTC)·d(GAGACTC*GAGAG) containing a single transplatin interstrand cross-link between complementary G and C residues determined using ^{1}H NMR spectroscopy and NMR-constrained molecular mechanics with the program JUMNA.

MATERIALS AND METHODS

Oligonucleotide platination and sample preparation

The two purified oligonucleotides d(CTCTCGAGTCTC) and d(GAGACTCGAGAG) were purchased from the Institut Pasteur (Paris). Preparation of the duplex containing a single *trans*-diammineplatinum interstrand cross-link was done as previously described (22,23) and can be summarized as follows (where ⌐●¬ represents the transplatin cross-link):

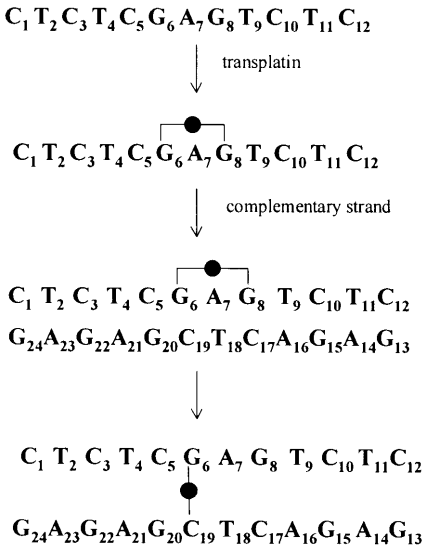

Briefly, the pyrimidine-rich strand was first reacted with transplatin. The platinated oligonucleotide containing a single 1,3-*trans*{Pt(NH_3)$_2$[d(GAG)]} intrastrand cross-link was then purified by strong anion exchange chromatography on a Pharmacia FPLC system equipped with a monoQ column. The molar amount of platinated oligonucleotide (Na^+ form) was deduced from its weight and from the UV absorbance of the sample resuspended in water (the effect of platination on the oligonucleotide extinction coefficient was neglected). Then, one molar equivalent of the complementary strand was added (the appropriate amount was determined according to both the UV absorbance of the oligonucleotide solution and the weight of the dried sample). The ratio between the two strands was further checked by strong anion exchange chromatography (22). Then, the duplex (3 µM final concentration) in 500 mM NaCl, 0.2 mM EDTA, 10 mM phosphate buffer, pH 7.5, was incubated at 20°C in the dark. Formation of the duplex triggered rearrangement of the intrastrand cross-link into an interstrand cross-link (22,23). The progress of the interstrand cross-linking reaction was monitored by FPLC on a monoQ column. After 2 weeks, the reaction was almost complete with duplexes containing an interstrand cross-link representing >95% of the reaction products. The reaction mixture was then desalted on a Sep-Pak column and then on a Chelex-100 column. The platinated duplex was used directly for NMR experiments without further purification.

NMR spectroscopy

The platinated duplex solution was lyophilized several times in D_2O and dissolved in D_2O containing 100 mM NaCl. The NMR sample (2 mM duplex) was degassed and kept in a sealed tube.

NMR experiments were carried out with a Bruker AMX500 spectrometer operating at 11.74 Tesla and processed on a X32 computer. Typically, spectra were recorded with 1024 complex data points in the domains t_1 and t_2. The data matrix was resolution enhanced by a Gaussian window function in direction 1. All D_2O experiments were recorded with the carrier frequency set to the HDO resonance, a weak presaturation, and a sweep width of 5001 and 5050 Hz in the F1 and F2 dimensions, respectively. For H_2O experiments, sweep widths of 7203 and 12 820 Hz were used in the F1 and F2 dimensions, respectively, and the last $\pi/2$ pulse was replaced by a jump and return selective excitation (24) in the NOESY spectra. Two-dimensional data sets for DQF-COSY, TOCSY and NOESY spectra were collected in the States mode (25). Clean TOCSY (26) experiments were recorded at 80 ms mixing time. For the 2-dimensional spectrum recorded in H_2O, the baseline was corrected following the procedure described by Marion *et al*. (27).

Four NOESY spectra in D_2O were run at 12°C with mixing times of 0, 80, 150 and 300 ms and were used to measure the NOE intensities. A NOESY spectrum with 600 ms mixing time was run at 20°C in D_2O for assignment and a NOESY spectrum with 300 ms mixing time was run at 13°C in H_2O, 10% D_2O for exchangeable proton assignment. These spectra were collected without removing the sample from the spectrometer or changing any frequency or gain. For each t_1 value, 64 scans were collected with a relaxation delay of 2.2 s between transients. The data used for distance calculations were not apodized with the t_2 dimension and were processed with a sine squared 90° phase-shifted function. This light apodization function did not distort the signal intensities, and the resulting peaks have no truncation effects.

Each NOE value was obtained by dividing the corresponding cross-peak volume by the diagonal peak volume obtained at 0 mixing time (28). The same processes were used to simulate the NOE via the complete relaxation matrix. The cross-peak volumes were calculated with the integration routines of the UXNMR software package (Bruker).

Molecular modeling

Modeling of the cross-linked duplex was performed using the internal coordinate program JUMNA (29). Based on a combination of internal and helical variables, this program permits important and efficient structural deformations during energy minimization. The transplatin residue was treated as a ligand coordinated to N7 of G_6* and N3 of C_{19}* through special types of bonding constraints on distances (N–Pt = 2.05 Å) (30,31), valence angles and dihedral angles to form an approximately square-planar complex. Special care was taken to conserve the Pt–N7 bond within the bisecting plane of the C5–N7–C8(G_6*) valence angle and the Pt–N3 bond within the bisecting plane of

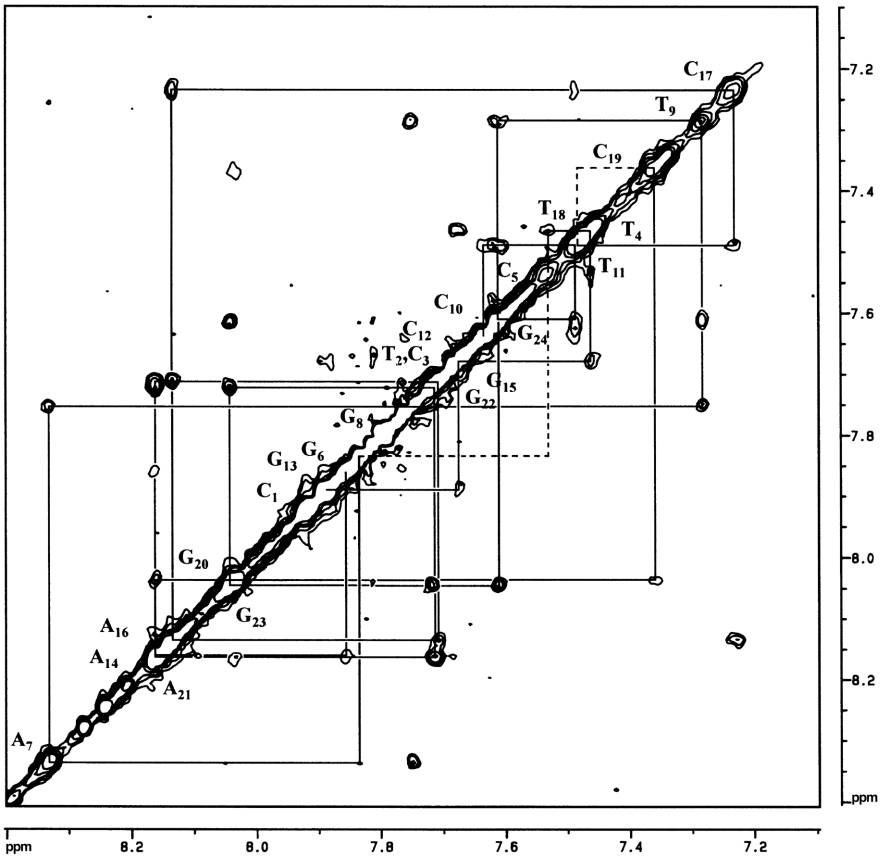

Figure 1. Expansion of the aromatic to aromatic proton region of the NOESY spectrum of the cross-linked duplex d(CTCTCG*AGTCTC)·d(GAGACTC*GAGAG) at 22°C in D_2O, with a mixing time of 300 ms. The full lines show the sequential assignment of the duplex and the dotted lines show the lack of connectivities C_5–G_6* and T_{18}–C_{19}*.

the C2–N3–C4(C_{19}*) valence angle. The N7(G_6*)–Pt–N3(C_{19}*) valence angle was constrained to 180°. The monopole charges of the cross-linked G* and C* and of the transplatin residue were in accordance with Prévost *et al*. (32).

An unknown distance d_{ij} between two protons giving rise to a NOE intensity can be determined from a reference distance d_{kl} using the following relationship:

$$d_{ij} = d_{kl}(NOE_{kl}/NOE_{ij})^{1/6} \quad \mathbf{1}$$

A suitable reference vector in nucleic acids is the cytosine H6–H5 vector, whose length is constant and known (2.46 Å). A global correlation time of 5.3 ns was obtained by fitting the experimental NOE values for the H6–H5 of cytosines for 80, 150 and 300 ms mixing times. The NOE intensities were converted into distances using the full relaxation matrix calculation (33). This approach has been incorporated in the RELAZ program (34) in which proton–proton distances are determined from a starting model of the structure. These distances are then introduced into the JUMNA program as distance constraints. After the first constrained energy minimization obtained with only the shorter distance constraints (≤3 Å), the resulting structure was used to compute new target distances according to the relation (34):

$$d_{new} = d_{old}(NOE_{calculated}/NOE_{observed})^{1/6} \quad \mathbf{2}$$

These new distances are iteratively updated until all the observed intensities agree with the corresponding calculated NOE intensities.

RESULTS AND DISCUSSION

NMR assignment of the non-exchangeable protons

Figures 1 and 2 show the NOESY spectra of the non-exchangeable protons of the cross-linked duplex d(CTCTCG*AGTCTC)·d(GAGACTC*GAGAG). All the non-exchangeable proton resonance lines (except H5′/H5″) were assigned and their chemical shifts are given in Table 1. The terminal complementary sequences $C_1T_2C_3T_4{\cdot}A_{21}G_{22}A_{23}G_{24}$ and $G_8T_9C_{10}T_{11}C_{12}{\cdot}G_{13}A_{14}G_{15}A_{16}C_{17}$ showed connectivities typically observed in a right-handed helix, i.e. the ones between the aromatic proton H6 or H8 and H1′ or H2″ of their 5′-neighbor as well as those between H5 of cytosine or CH3 of thymine and the H6 or H8 protons of the 5′-neighboring nucleotide. However, several anomalies were observed for the connectivities expected between the cross-linked G_6* or C_{19}* and their adjacent neighbors, indicating the presence of structural features not present in B-DNA.

For all the mixing times used, the H8–H1′ cross-peak of G_6* was much stronger than all the other cross-peaks (Fig. 2). Because the distance between the ring H8 and the sugar H1′ proton does not depend on the sugar conformation but only on

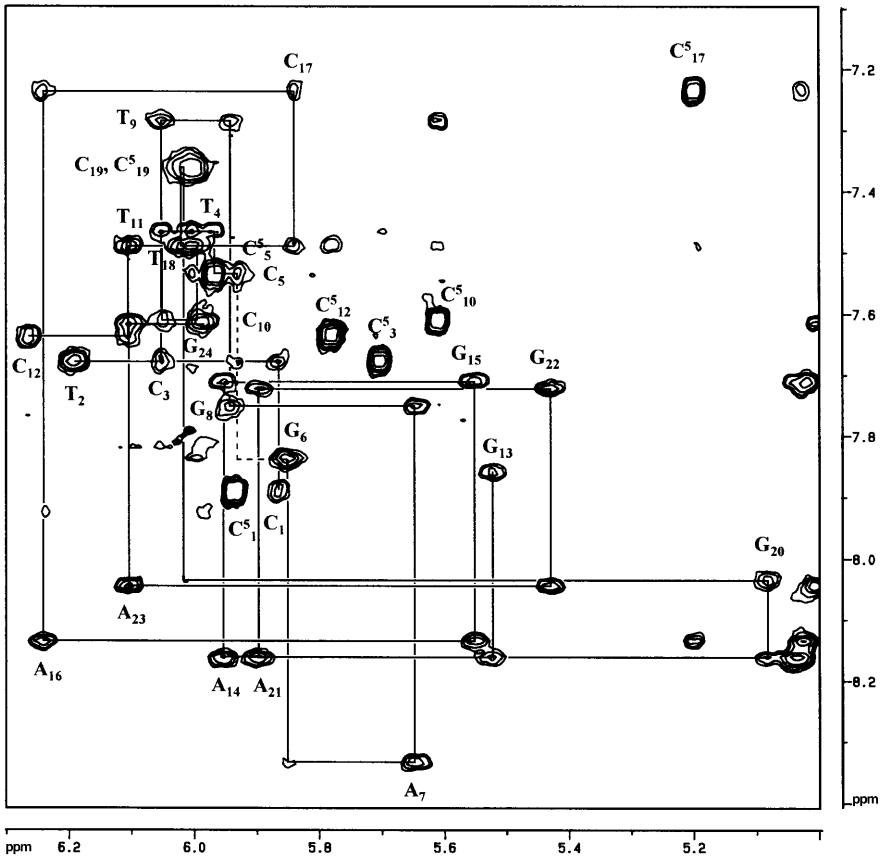

Figure 2. Expansion of the aromatic to H1′ and aromatic to H5 (of the cytosines) proton region of the NOESY spectrum of the cross-linked duplex d(CTCTCG*AGTCTC)·d(GAGACTC*GAGAG) at 22°C in D_2O, with a mixing time of 300 ms. The full lines show the sequential assignment of the duplex and the dotted line shows the lack of connectivity between C_5 and G_6* residues. Notice the very weak connectivities C_{19}*–G_{20} and G_6*–A_7, and the strong upfield shift of H1′(G_{20}). The existence of the connectivity between T_{18} and C_{19}* was impossible to determine due to the overlap with H5(C_{19}*) and H6(C_{19}*).

the glycosidic torsion angle (35), this result implies a *syn* conformation of G_6*.

The absence of the base–base NOEs H6(C_5)–H8(G_6*) and H6(T_{18})–H6(C_{19}*) and the weakness of the base–base NOEs H8(G_6*)–H8(A_7) and H8(G_{20})–H6(C_{19}*) (Fig. 1) indicated large distances separating the base pairs. These data were confirmed by the absence of NOEs between H1′/H2′/H2″(G_6*) and H6(C_5) as well as between H1′/H2′/H2″(C_6) and H6(T_7).

In addition, unusual chemical shifts were observed for residues 5–8 (Table 1). The resonance position of a particular proton in a molecule is in essence determined by its chemical environment. In a DNA double helix, the direct environment of any particular proton is determined by the nucleotide sequence which itself affects the local conformation. For example, stacking of bases induces an upfield shift of the corresponding resonances. Here, we notice a downfield shift of H5(C_5), H8(G_{20}), H8(G_6*) and H6(T_{18}), and an upfield shift of many protons: H2′/H2″(C_5), H1′(G_{20}), H3′(G_6*), H6/H2′/H2″(C_{19}*), H5/H6/H2′(C_{17}) and CH_3/H6(T_9). This reflects irregularities in the stacking of base pairs 5–8.

NMR assignment of the exchangeable protons

Because of significant overlap, only a few imino–imino connectivities could be determined from the NOESY spectra of exchangeable protons. However, the ^{1}H NMR 1-dimensional spectrum permitted the assignment of all the imino protons (Fig. 3) with the exception of H1(G_6*) (Table 1). The data support the presence of Watson–Crick base pairs although the terminal residues G_{24}, T_2 and G_{13} and the central one G_{20} are involved in fast chemical exchange. The region near the cross-link appears to offer large accessibility to solvent. The imino proton of G_6* could not be assigned because of a very fast chemical exchange. This is consistent with its location in the major groove due to the *syn* conformation of G_6*.

Several cross-peaks were detected between amino protons of cytosines and imino protons of their paired guanines as well as between H_2 protons of adenines and imino protons of their paired thymines. Therefore, Watson–Crick pairings C_1–G_{24}, T_2–A_{23}, C_3–G_{22}, T_4–A_{21}, G_8–C_{17}, T_9–A_{16}, C_{10}–G_{15}, T_{11}–A_{14} and C_{12}–G_{13} could be confirmed. Connectivities between amino protons of cytosines and CH_3 of their 5′-neighboring thymines were also detected, except between C_{19}* and T_{18}.

Other anomalies were observed in the spectra in H_2O. The amino protons of the cross-linked C_{19}* had chemical shifts of 7.37 and 7.26 p.p.m., respectively. These chemical shifts are slightly downfield shifted as compared to the ones corresponding to non-hydrogen bonded protons (6.76–7.10 p.p.m.) and are characteristic of a weakly paired cytosine or a cytosine involved in a hydrogen bond arrangement different from Watson–Crick pairing. Finally, amino protons of C_5, readily

Table 1. Assignment of the non-exchangeable protons at 20°C (600 ms mixing time NOESY) and the exchangeable protons at 13°C of the cross-linked duplex d(CTCTCG*AGTCTC)·d(GAGACTC*GAGAG)

	H8/H6	H2/H5/CH3	H1′	H2′	H2″	H3′	H4′	Hb	Hf	H1/H3
C_1	7.89	5.94	5.86	2.25	2.59	4.66	4.10	7.90	7.10	
T_2	7.67	1.68	6.19	2.34	2.62	4.93	4.30			13.98
C_3	7.67	5.51	6.05	2.22	2.61	4.83	4.22	8.41	7.13	
T_4	7.46	1.72	6.00	2.04	2.40	4.85	4.13			14.01
C_5	7.53	5.97	5.93	1.83	1.86	4.80	4.06	8.41	7.49	
G_6*	7.83		5.85	2.23	2.54	4.32	4.19			
A_7	8.33	7.47	5.65	2.78	2.73	4.93	4.32			
G_8	7.75		5.94	2.55	2.73	4.89	4.37			12.65
T_9	7.28	1.28	6.05	2.21	2.54	4.88	4.24			13.62
C_{10}	7.61	5.61	5.99	2.35	2.53	4.76	4.19	8.29	6.97	
T_{11}	7.49	1.71	6.11	2.17	2.52	4.88	4.17			13.62
C_{12}	7.63	5.78	6.27	2.28	2.28	4.57	4.01	8.21	7.10	
G_{24}	7.61		5.99	2.25	2.38	4.61	4.16			12.42
A_{23}	8.04	7.80	6.11	2.60	2.88	5.01	4.41			
G_{22}	7.72		5.43	2.56	2.66	4.97	4.31			12.65
A_{21}	8.16	7.64	5.90	2.71	2.81	5.02	4.35			
G_{20}	8.03		5.08	2.63	2.63	4.89	4.19			12.80
C_{19}*	7.36	6.01	6.01	1.79	2.22	4.75	4.09	7.37	7.26	
T_{18}	7.49	1.74	6.02	2.08	2.31	4.91	4.10			12.63
C_{17}	7.23	5.20	5.84	1.88	2.41	4.75	4.15	7.88	6.76	
A_{16}	8.14	7.83	6.24	2.69	2.91	5.03	4.49			
G_{15}	7.71		5.55	2.60	2.72	5.02	4.39			12.63
A_{14}	8.16	7.74	5.95	2.73	2.86	5.05	4.40			
G_{13}	7.86		5.52	2.47	2.66	4.80	4.15			13.28

Hb and Hf represent the bonded and free amino protons $N4H_2$.

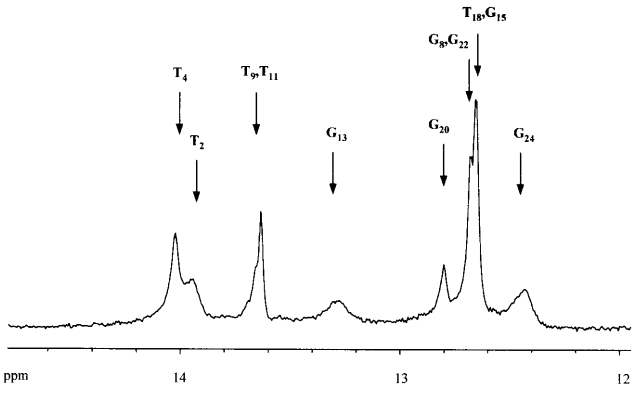

Figure 3. Imino proton resonances of the cross-linked duplex d(CTCTCG*AGTCTC)·d(GAGACTC*GAGAG) at 13°C in 90% H_2O, 10% D_2O.

assigned from their NOEs to the aromatic proton H5, have slightly upfield shifted chemical shifts of 8.41 and 7.49 p.p.m.

Structural features of the interstrand cross-linked duplex

In addition to NOE-derived restraints on distances, a large number of restraints on valence or dihedral angles, sugar phases and amplitudes were deduced from NMR data and used for structure determination with the JUMNA program. All sugars are constrained to be in the south conformation with a pseudorotation phase angle in the range 140–190° and an amplitude of 30–40°. This is deduced from H1′–H4′ distances of every sugar moiety and the H1′–H2′/H1′–H2″ cross-peaks observed for all the residues in the COSY spectrum.

Energy minimization was performed with 330 constraints and, after three iterations, the overall process (see Materials and Methods) resulted in a reasonable agreement between the calculated distances and all the inter-proton distances constituting the constrained database. An NMR *R*-factor of 17% was obtained. Our constrained molecular mechanics calculation led to structures belonging to the same family. The average refined structure is shown in Figure 4.

The structural properties were analyzed using the CURVES algorithm (36). The distortion induced by the platinum moiety is restricted to the cross-linked bases and their adjacent

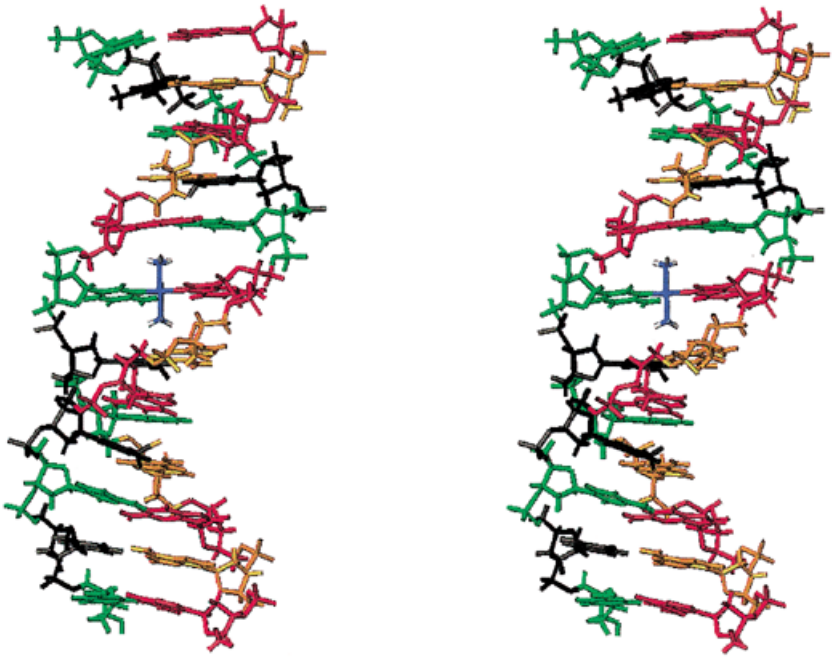

Figure 4. Stereo view of the solution structure of the cross-linked duplex d(CTCTCG*AGTCTC)·d(GAGACTC*GAGAG) generated with the program MOLMOL (43). The residue color code is: blue, platinum; green, cytosine; red, guanine; black, thymine; orange, adenine.

Table 2. Base pair parameters as given by the program CURVES

	Rise per base pair (Å)	Helix twist angle (°)
C_1–G_{24}/T_2–A_{23}	4.1	38.3
T_2–A_{23}/C_3–G_{22}	3.9	35.3
C_3–G_{22}/T_4–A_{21}	2.9	39.4
T_4–A_{21}/C_5–G_{20}	3.0	29.2
C_5–G_{20}/G_6*–C_{19}*	5.3	41.2
G_6*–C_{19}*/A_7–T_{18}	5.1	41.0
A_7–T_{18}/G_8–C_{17}	3.7	29.2
G_8–C_{17}/T_9–A_{16}	3.3	38.3
T_9–A_{16}/C_{10}–G_{15}	3.6	32.8
C_{10}–G_{15}/T_{11}–A_{14}	3.2	38.7
T_{11}–A_{14}/C_{12}–G_{13}	3.1	37.4

neighbors, the rest of the duplex adopting a B-conformation. Base pair parameters obtained with the program CURVES are listed in Table 2. There is an increased rise between C_5–G_{20}/G_6*–C_{19}* (5.3 Å) and G_6*–C_{19}*/A_7–T_{18} (5.1 Å). The platinum ammine groups are placed above and below the planes of the cross-linked residues, and interact with the adjacent base pairs, pushing them away along the axis of the double helix. The average twist angle value (ω = 36.4°) is close to the B-conformation value, and thus no global unwinding is found for the whole duplex, although unwinding and overwinding values are found from T_4 to G_8 (Table 2).

The platinated residue G_6* adopts a *syn* conformation (χ = 47°), whereas all the other residues are in the *anti* conformation (–100° < χ < –121°). The platinated G_6* is rotated around the N7(G_6*)–N3(C_{19}*) axis with a propeller twist of 166°. This has already been observed in the crystals of methylated guanine and cytosine residues cross-linked by transplatin (37). The rotation resulted in a Hoogsteen-type pairing of G_6* and C_{19}* constrained by the metal chelation and stabilized by a hydrogen bond between O6(G_6*) and N4H(C_{19}*) (Fig. 5).

The local distortion induced by the transplatin cross-link slightly affects the conformation of the sugar rings of C_5 which is C1′-*exo* (P = 138°), and of A_7 and C_{19}* which are C3′-*exo* (P = 185° and 181°, respectively). All other sugars adopt a C2′-*endo* conformation (148° < P < 179°). Some alteration in the torsion angle values have also been determined by CURVES, especially the α (P–O5′) and γ (C5′–C4′) angles for C_5, G_6*, A_7, T_{18} and C_{19}*. The platinated duplex is slightly bent by ~20° toward the minor groove.

CONCLUSION

The NMR study reported here provides the first high resolution structure of a DNA helix containing a transplatin interstrand cross-link between complementary G and C residues, this adduct being the major bifunctional adduct formed in the reaction between double-stranded DNA and transplatin (15). It confirms and extends our previous analysis of a DNA duplex containing a single transplatin interstrand cross-link which was conducted with conventional biochemical approaches (21). For instance, it unambiguously proves the *syn* conformation of the cross-linked G residue. It indicates that the helix is slightly bent (20°) towards the minor groove. The whole double helix

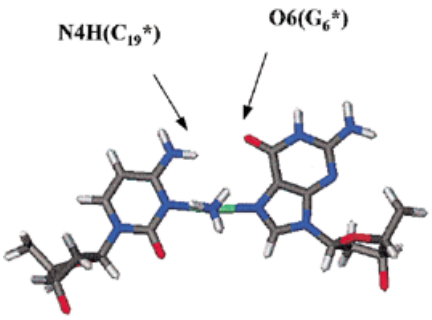

Figure 5. View of the platinated C_{19}*–G_6* base pair. Both platinated amino groups are located perpendicular to the plane formed by the cross-linked G_6* and C_{19}* bases. The *syn* conformation of G_6* resulted in a Hoogsteen type pairing of G_6* and C_{19}* stabilized by a hydrogen bond between O6(G_6*) and N4H(C_{19}*). The atom color code is: blue, N; grey, C; red, O; pale green, Pt; light grey, H.

does not seem to be unwound whereas the electrophoretic mobility data suggest a short unwinding (12°). Although the discrepancy may reflect inaccuracy in one or both methods, it also rules out a large unwinding of the helix resulting from the presence of a transplatin interstrand cross-link. The distortion induced by the cross-link spreads over 2 bp on the 5′- and 3′-sides of the complex. These complementary nucleotides are paired but as compared to B-DNA, the puckering of the sugars and the twist angles are changed.

An interesting point concerns the location of the ammine groups of the transplatin residue. In crystal structures of transplatin-modified nucleobases it has been found that the ammine groups have different locations but can be close to the nucleobases and leave the stacking interaction almost unchanged (38,39). In the transplatin-modified duplex the ammine groups are above and below the plane of the cross-linked residues, respectively, interact with the adjacent base pairs and push them away along the axis of the double helix. This could explain, at least in part, the slow closure of the monofunctional adduct into an interstrand cross-link ($t_{1/2}$ > 17 h). In order to locate the platinum residue near the N3 of the cytosine residue complementary to the monofunctional adduct, two events have to occur concomitantly, i.e. rotation of the platinated guanine residue from the *anti* to the *syn* conformation and displacement of the adjacent base pairs along the axis of the double helix. Along these lines, one expects the rate of the interstrand cross-linking reaction to be sensitive to local conformational modifications of the DNA double helix. This can be achieved in several ways. In addition to the effects of salt and temperature on melting of the duplex and/or the presence of adducts in the vicinity of the reactive species (17), one way is to replace the monofunctional *trans*-$[Pt(NH_3)_2(dG)Cl]^+$ adduct by the monofunctional *trans*-$[Pt(NH_3)_2(dC)Cl]^+$ adduct. It is likely that the monofunctional *trans*-$[Pt(NH_3)_2(dC)Cl]^+$ adduct is no longer paired with the complementary G residue. Unpairing of the G residue facilitates its rotation to the *syn* conformation and insertion of the monofunctional *trans*-$[Pt(NH_3)_2(dC)Cl]^+$ adduct into the double helix. Indeed, closure of the monofunctional *trans*-$[Pt(NH_3)_2(dC)Cl]^+$ adduct into an interstrand cross-link is relatively fast ($t_{1/2}$ = 2–3 h) (to be published). Another way is to change the chemical nature of the non-leaving groups of the platinum residues. The interaction between the non-leaving groups and the adjacent nucleotides can stabilize or destabilize the double helix. As compared to transplatin, *trans*-$[PtCl_2(NH_3)$-(quinoline)] forms more interstrand cross-links and the reaction is faster ($t_{1/2}$ = 5 h) whereas *trans*-$[PtCl_2$(E-iminoether)$_2]$ forms fewer interstrand cross-links and the reaction is slower (40–42).

A final comment concerns rearrangement of the transplatin (G1,G3) intrastrand cross-links into interstrand cross-links. The (G1,G3) intrastrand cross-links are formed in the reaction between transplatin and the sequence GNG within single-stranded oligonucleotides but not within double-stranded oligonucleotides. Pairing of the platinated single-stranded oligonucleotides with their complementary strands promotes rearrangement of the intrastrand cross-links into interstrand cross-links. The rate of rearrangement and the nature of the resulting interstrand cross-links depend upon several parameters (8,24). For example, replacement of the triplet facing the intrastrand cross-link by a TA or UA doublet increases the rate of rearrangement and G1 is cross-linked to A and no longer to the complementary C. Knowledge of the structure reported here and that of a DNA 12/11mer containing a transplatin interstrand cross-link G–A (B.Andersen, E.Bernal-Mendez, M.Leng and E.Sletten, in preparation) should help in our understanding of the mechanism of the linkage isomerization reaction and in designing platinum(II) complexes that favor a faster reaction.

ACKNOWLEDGEMENTS

We would like to thank R. Lavery for providing the JUMNA software. We are indebted to Professor E. Sletten (Bergen) for helpful discussions. This work was supported in part by la Ligue contre le Cancer, l'Association Nationale de Recherches sur le Sida and EU contracts (Cost D8 and BMH4-CT97-2485).

REFERENCES

1. Barry,M.A., Behnke,C.A. and Eastman,A. (1990) *Biochem. Pharmacol.*, **40**, 2353–2362.
2. Chu,G. (1994) *J. Biol. Chem.*, **269**, 787–789.
3. Henkels,K.M. and Turchi,J.J. (1997) *Cancer Res.*, **57**, 4488–4492.
4. Comess,K.M. and Lippard,S.J. (1993) In Neidle,S. and Waring,M. (eds), *Molecular Aspects of Anti-cancer Drug–DNA Interactions*. Macmillan, London, UK, pp. 134–168.
5. Sip,M. and Leng,M. (1993) In Eckstein,F. and Lilley,D.M.J. (eds), *Nucleic Acids and Molecular Biology*. Springer-Verlag, Berlin, Germany, pp. 1–15.
6. Reedijk,J. (1996) *Chem. Commun.*, 801–806.
7. Zamble,D.B. and Lippard,S.J. (1999) The response of cellular proteins to cisplatin-damaged DNA. In Lippert,B. (ed.), *Cisplatin: Chemistry and Biochemistry of a Leading Anticancer Drug*. Wiley-VCH, Zurich, Switzerland, pp. 73–110.
8. Malinge,J.M. and Leng,M. (1999) Interstrand cross-links in cisplatin or transplatin-modified DNA. In Lippert,B. (ed.), *Cisplatin: Chemistry and Biochemistry of a Leading Anticancer Drug*. Wiley-VCH, Zurich, Switzerland, pp. 159–180.
9. Farrell,N., Kelland,L.R., Roberts,J.D. and van Beusichem,M. (1992) *Cancer Res.*, **52**, 5065–5072.
10. Zou,Y., Van Houten,B. and Farrell,N. (1993) *Biochemistry*, **32**, 9632–9638.
11. Coluccia,M., Nassi,A., Loseto,F., Boccarelli,A., Mariggio,M.A., Giordano,D., Intini,F.P., Caputo,P. and Natile,G. (1993) *J. Med. Chem.*, **36**, 510–512.
12. Coluccia,M., Boccarelli,A., Mariggio,M.A., Cardellicchio,N., Caputo,P., Intini,F.P. and Natile,G. (1995) *Chem. Biol. Interact.*, **98**, 251–266.

13. Kelland,L.R., Barnard,C.F., Evans,I.G., Murrer,B.A., Theobald,B.R., Wyer,S.B., Goddard,P.M., Jones,M., Valenti,M. and Bryant,A. (1995) *J. Med. Chem.*, **38**, 3016–3024.
14. Qu,Y., Bloemink,M.J., Reedijk,J., Hambley,T.W. and Farrell,N. (1996) *J. Am. Chem. Soc.*, **118**, 9307–9313.
15. Brabec,V. and Leng,M. (1993) *Proc. Natl Acad. Sci. USA*, **90**, 11676–11681.
16. Boudvillain,M., Dalbies,R., Aussourd,C. and Leng,M. (1995) *Nucleic Acids Res.*, **23**, 2381–2388.
17. Bernal-Mendez,E., Boudvillain,M., Gonzalez-Vilchez,F. and Leng,M. (1997) *Biochemistry*, **36**, 7281–7287.
18. Huang,H., Zhu,L., Reid,B.R., Drobny,G.P. and Hopkins,P.B. (1995) *Science*, **270**, 1842–1845.
19. Paquet,F., Perez,C., Leng,M., Lancelot,G. and Malinge,J.M. (1996) *J. Biomol. Struct. Dyn.*, **14**, 67–77.
20. Coste,F., Malinge,J.M., Serre,L., Sheppard,W., Roth,M., Leng,M. and Zelwer,C. (1999) *Nucleic Acids Res.*, **27**, 1837–1846.
21. Brabec,V., Sip,M. and Leng,M. (1993) *Biochemistry*, **32**, 11676–11681.
22. Dalbies,R., Payet,D. and Leng,M. (1994) *Proc. Natl Acad. Sci. USA*, **91**, 8147–8151.
23. Boudvillain,M., Guerin,M., Dalbies,R., Saison-Behmoaras,T. and Leng,M. (1997) *Biochemistry*, **36**, 2925–2931.
24. Plateau,P. and Guéron,M. (1982) *J. Am. Chem. Soc.*, **104**, 7310–7311.
25. States,D.J., Haberkorn,R.A. and Ruben,D.J. (1982) *J. Magn. Reson.*, **48**, 286–292.
26. Griesinger,C., Otting,G., Wüthrich,K. and Ernst,R.R. (1988) *J. Am. Chem. Soc.*, **110**, 7870–7872.
27. Marion,D., Ikura,A.M. and Bax,A. (1989) *J. Magn. Reson.*, **84**, 425–430.
28. Cavanagh,J., Fairbrother,W.J., Palmer,A.G. and Skelton,N.J. (1996) In *Protein NMR Spectroscopy—Principles and Practice*. Academic Press, New York, NY, pp. 386–389.
29. Lavery,R. (1988) In Olson,W.K., Sarma,R.H., Sarma,M.H. and Sundaralingam,M. (eds), *Structure and Expression—DNA Bending and Curvature*. Adenine Press, New York, NY, Vol. III, pp. 191–211.
30. Admiraal,G., van der Veer,J.L., de Graaff,R.A.G., den Hartog,J.H.J. and Reedijk,J. (1987) *J. Am. Chem. Soc.*, **109**, 592–594.
31. Coll,M., Sherman,S.E., Gibson,D., Lippard,S.J. and Wang,A.H.J. (1990) *J. Biomol. Struct. Dyn.*, **8**, 315–330.
32. Prévost,C., Boudvillain,M., Beudaert,P., Leng,M., Lavery,R. and Vovelle,F. (1997) *J. Biomol. Struct. Dyn.*, **14**, 703–714.
33. Barsukov,I. and Lian,L.Y. (1993) In Roberts,G.C.K. (ed.), *NMR of Macromolecules—A Practical Approach*. IRL Press, Oxford, UK, pp. 315–357.
34. Lancelot,G., Guesnet,J.L. and Vovelle,F. (1989) *Biochemistry*, **28**, 7871–7878.
35. Wijmenga,S.S., Mooren,M.M.W. and Hilbers,C.W. (1993) In Roberts,G.C.K. (ed.), *NMR of Macromolecules—A Practical Approach*. IRL Press, Oxford, UK, pp. 216–288.
36. Lavery,R. and Sklenar,H. (1989) *J. Biomol. Struct. Dyn.*, **6**, 655–667.
37. Dieter-Wurm,I., Sabat,M. and Lippert,B. (1992) *J. Am. Chem. Soc.*, **114**, 357–359.
38. Zamora,F., Witkowski,H., Freisinger,E., Müller,J., Thormann,B., Albinati,A. and Lippert,B. (1999) *J. Chem. Soc. Dalton Trans.*, 175–182.
39. Sigel,R.K.O., Sabat,M., Freisinger,E., Mower,A. and Lippert,B. (1998) *Inorg. Chem.*, **38**, 1481–1490.
40. Zakovska,A., Novakova,O., Balcarova,Z., Bierbach,U., Farrell,N. and Brabec,V. (1998) *Eur. J. Biochem.*, **254**, 547–557.
41. Zaludova,R., Zakovska,A., Kasparkova,J., Balcarova,Z., Vrana,O., Coluccia,M., Natile,G. and Brabec,V. (1997) *Mol. Pharmacol.*, **52**, 354–361.
42. Boccarelli,A., Coluccia,M., Intini,F.P., Natile,G., Locker,D. and Leng,M. (1999) *Anti-Cancer Drug Des.*, **4**, 253–264.
43. Koradi,R., Billeter,M. and Wüthrich,K. (1996) *J. Mol. Graph.*, **14**, 51–55.